ARCHIVES OF ACOUSTICS
20, 2, 191–205(1995)

NUMERICAL MODEL OF MULTIPLE SOUND SCATTERING FROM GAS BUBBLES IN THE SEA

J. SZCZUCKA

Institute of Oceanology
Polish Academy of Science
(81-712 Sopot, ul. Powstańców Warszawy 55)

This paper presents a model of sound scattering on gas bubbles aggregations in water. Coherence and second order scattering effects are taken into account for random and regular 3-dimensional distributions of bubbles with different parameters like bubble size, average separation between scatterers, distance to the receiver, incident sound frequency. Results of calculations for various sets of parameters are compared. Excess attenuation is also considered.

1. Introduction

Different objects enclosed in the sea water can be detected and counted by the sound scattering methods. Gas bubbles floating in the upper sea layer are generated mainly by breaking wind waves and by biological sources (photosynthesis, decaying organic matter). These bubbles play an important role in the ocean-atmosphere gas exchange. On the other hand they strongly influence the conditions of sound propagation in the sea, scattering and absorbing acoustic energy and changing the sound velocity. The intensity of all these processes depends on the concentration of microbubbles, which can be measured by means of acoustic methods, similar to fish counting. The majority of these methods is based on two fundamental assumptions concerning *single scattering* — that is equivalent to the noninteraction between scatterers — and *incoherent scattering* — the total intensity of backscattered sound is treated as a sum of intensities originating from the individual centres. If the discrete scatterers are distributed in space randomly and not too densely, these assumptions can be sufficient for solving the problem of backscattering, but in some circumstances depending on the wavelength, distance between scattering centres, distance between receiver and scatterers, they can oversimplify the real sitaution and lead to significant errors, therefore this problem should be taken into consideration in each individual case.

Most of scattering models applied to marine inhomogeneities ignore the effects of coherence and multiple scattering, but these effects were considered by some authors

using different simplifying assumptions. KURIANOV [3] showed analytically, that coherent scattering of the time-limited acoustic pulse on the set of randomly distributed objects can be neglected. STANTON [5, 6] evaluated the second order effects for scattering on clouds of identical randomly distributed isotropic scatterers under the following assumptions: the average distance between individual objects was much greater than the acoustic wavelength (the short wavelength limit), the swarm of scatterers was located in the plane-wave region of the transceiver and absorption was negligible. Under these conditions, second order scattering was shown to play an important role, especially in the case of using multibeam sonars. BRUNO and NOVARINI [1] considered both coherence and interaction effects, but only for 1-dimensional (linear) distributions of gas-filled bubbles.

In this paper the mathematical model of acoustic backscattering of spherical wave from the aggregation of gas bubbles in water has been considered. The expressions for the coherent and incoherent terms of the first and second order of the backscattered energy have been obtained. The model was used for both random and regular 3-dimensional distributions of gas bubbles with the same radii or with given size spectrum, for various densities and various distances to the receiver, with the attenuation included or not.

2. Scattering and attenuation by a single gas bubble

For the acoustic wave of frequency f the function of backscattering t_j on a gas bubble with the radius a_j is given by [4, 7]:

$$t_j = \frac{a_j}{(f_{Rj}/f)^2 - 1 + i\delta_j}, \tag{2.1}$$

where δ_j is a damping constant of the jth bubble, depending on the bubble size, incident sound frequency and number of physicochemical parameters of the gas and sea water, and f_{Rj} is its resonant frequency

$$f_R = \frac{\sqrt{3\gamma P/\rho}}{2\pi a}, \tag{2.2}$$

where γ — the ratio of specific heats of gas, P — hydrostatic pressure at given depth, ρ — water density. Taking the complex function t_j in the form

$$t_j = \rho_j \exp(i\varphi_j), \tag{2.3}$$

we get

$$\rho_j = \frac{a_j}{\sqrt{[(f_{Rj}/f)^2 - 1]^2 + \delta_j^2}}, \tag{2.4}$$

$$\tan\varphi_j = -\frac{\delta_j}{(f_{Rj}/f)^2 - 1}.$$

There is the following relationship between the backscattering function and backscattering cross-section of a gas bubble [4, 7]:

$$\sigma_{bs} = |f|^2 = \frac{a_j^2}{[(f_{Rj}/f)^2 - 1]^2 + \delta_j^2}. \tag{2.5}$$

Extinction cross-section of a gas bubble looks similar:

$$\sigma_e = \frac{4\pi a_j^2 (\delta_j / k a_j)}{[(f_{Rj}/f)^2 - 1]^2 + \delta_j^2} \tag{2.6}$$

At resonance bubble cross-sections are reduced to:

$$\sigma_{bs,R} = a_j^2/\delta_j^2$$
$$\sigma_{e,R} = 4\pi a_j/k\delta_j \tag{2.7}$$

The dependence of ρ, φ and δ on frequency for air bubble with radius 100 μm is displayed in Fig. 1.

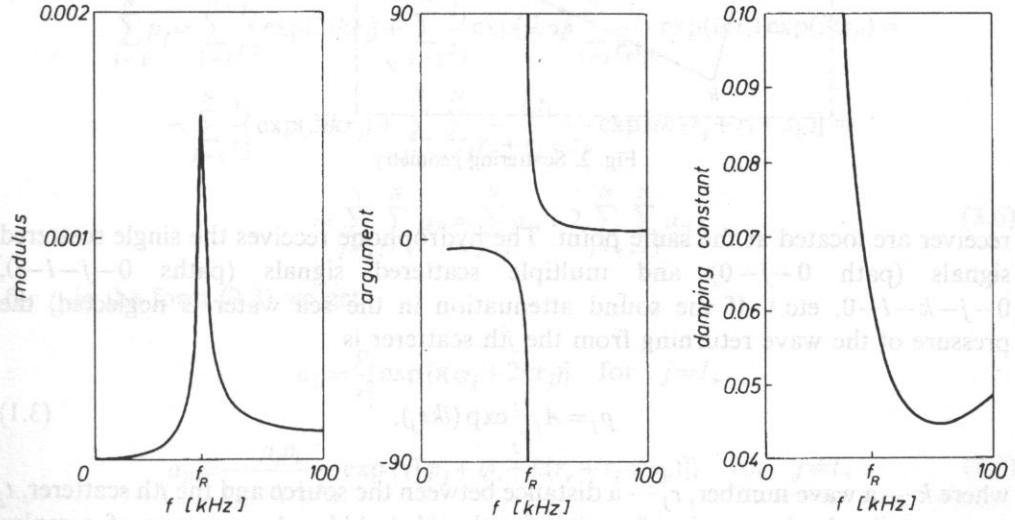

Fig. 1. Dependence of the modulus and argument of backscattering function and damping constant on frequency of incident sound for air bubble with radius $a = 100$ μm located at depth $z_0 = 10$ m.

3. Scattering model without attenuation

Let us consider the problem of backscattering of the spherical sound wave on the aggregation of N gas bubbles enclosed in any volume V with the centre at a depth z_0 related to the source depth (Fig. 2). The geometry is monostatic — source and

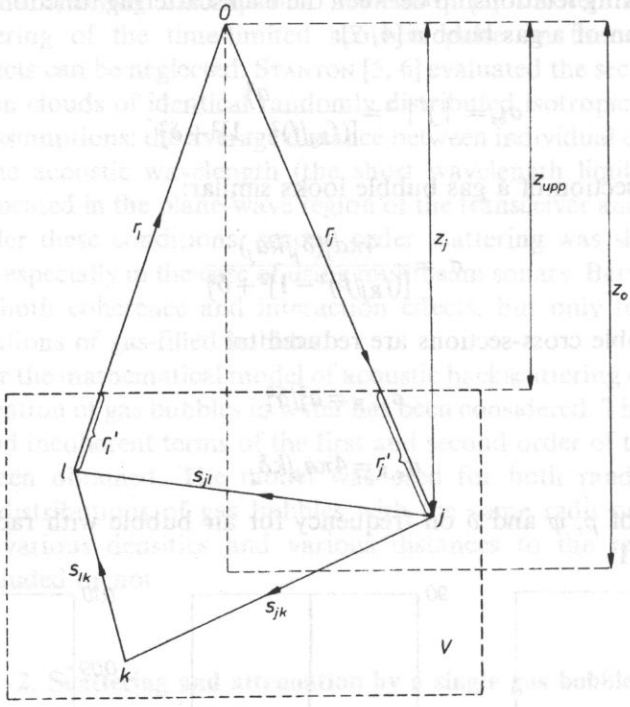

Fig. 2. Scattering geometry

receiver are located at the same point. The hydrophone receives the single scattered signals (path $0-j-0$) and multiple scattered signals (paths $0-j-l-0$, $0-j-k-l-0$, etc.). If the sound attenuation in the sea water is neglected, the pressure of the wave returning from the jth scatterer is

$$p_j = A_j \frac{t_j}{r_j} \exp(ikr_j), \tag{3.1}$$

where k — a wave number, r_j — a distance between the source and the jth scatterer, t_j — a complex backscattering function for the jth bubble, A_j — a sum of complex amplitudes of the spherical waves coming to the jth scatterer from all other bubbles

$$A_j = A_{0j} + \sum_{l \neq j}^{N} A_l \frac{t_l}{s_{jl}} \exp(iks_{jl}). \tag{3.2}$$

In this formula s_{jl} is a distance from the jth to lth scattering object and A_{0j} is an amplitude of the spherical wave coming to the jth scatterer directly from the source

$$A_{0j} = \frac{A_0}{r_j} \exp(ikr_j), \tag{3.3}$$

where A_0 is an amplitude of the wave emitted from the source.

The expression (3.2) is a reccurence formula including scattering effects to all orders. In the presented model it is assumed $A_l = A_{0l}$, what is a consequence of neglecting all the effects over the second order, and for simplicity, $A_0 = 1$. According to the fundamental hypothesis, in practice we measure an incoherent field of single scattered signals:

$$I_{\text{in}} = \sum_{j=1}^{N} | p_j^{(1)} |^2, \tag{3.4}$$

but in fact we measure a total field (including coherent terms) of multiple scattered signals:

$$I_{\text{tot}} = \left| \sum_{j=1}^{N} p_j \right|^2. \tag{3.5}$$

The main goal of calculations is a total intensity with taking phase relations into account, therefore the coherent sum of pressure is needed:

$$\sum_{j=1}^{N} p_j = \sum_{j=1}^{N} \frac{t_j}{r_j^2} \exp(2ikr_j) + \sum_{j=1}^{N} \frac{t_j}{r_j} \exp(ikr_j) \sum_{l \neq j}^{N} \frac{t_l}{r_l s_{jl}} \exp(ikr_l) \exp(iks_{jl}) =$$

$$= \sum_{j=1}^{N} \frac{t_j}{r_j^2} \exp(2ikr_j) + \sum_{j=1}^{N} \sum_{l \neq j}^{N} \frac{t_j t_l}{r_j + r_l + s_{jl}} \exp[ik(r_j + r_l + s_{jl})] =$$

$$= \sum_{j=1}^{N} \sum_{l=1}^{N} a_{jl} = \sum_{j=1}^{N} a_{jj} + 2 \sum_{j=1}^{N} \sum_{l>j}^{N} a_{jl}. \tag{3.6}$$

for t_j in the form (2.3) we get

$$a_{jj} = \frac{\rho_j}{r_j^2} \exp[i(\varphi_j + 2kr_j)] \quad \text{for} \quad j = l,$$

$$a_{jl} = \frac{\rho_j \rho_l}{r_j + r_l + s_{jl}} \exp\{i[\varphi_j + \varphi_l + k(r_k + r_l + s_{jl})]\} \quad \text{for} \quad j \neq l, \tag{3.7}$$

The total scattered field is:

$$I_{\text{tot}} = \left| \sum_{j=1}^{N} p_j \right|^2 = \left(\sum_{j=1}^{N} p_j \right) \cdot \left(\sum_{j=1}^{N} p_j \right)^* = \sum_{j=1}^{N} \sum_{k=1}^{N} a_{jk} \cdot \sum_{l=1}^{N} \sum_{m=1}^{N} a_{lm}^*. \tag{3.8}$$

The product of these two sums comprises $N(N+1)/2$ incoherent terms $a_{jk} a_{jk}^* = | a_{jk} |^2$, where $j = l$, $k = m$, and $N(N+1)[N(N+1)/2 - 1]/4$ coherent terms $a_{jk} a_{lm}^* + a_{jk}^* a_{lm}$ involving phases. As a result w obtain:

$$I_{\text{tot}} = I_{\text{in}}^{(1)} + I_{\text{coh}}^{(1)} + I_{\text{in}}^{(2)} + I_{\text{coh}}^{(2)}, \tag{3.9}$$

where

$$I_{\text{in}}^{(1)} = \sum_{j=1}^{N} | a_{jj} |^2$$

$$I_{\text{coh}}^{(1)} = 2 \sum_{j=1}^{N} \sum_{l>j}^{N} | a_{jj} \| a_{ll} | \cos[\varphi_j - \varphi_l + 2k(r_j - r_l)]$$

$$I_{\text{in}}^{(2)} = 4 \sum_{j=1}^{N} \sum_{k>j}^{N} | a_{jk} |^2$$

$$I_{\text{coh}}^{(2)} = 4 \sum_{j=1}^{N} \sum_{l=1}^{N} \sum_{m>l}^{N} | a_{jj} \| a_{lm} | \cos[\varphi_j - \varphi_l - \varphi_m + k(2r_j - r_l - r_m - s_{lm})] +$$

$$+ 8 \sum_{j=1}^{N} \sum_{k>j}^{N} \sum_{l=1}^{N} \sum_{m>l}^{N} | a_{jk} \| a_{lm} | \cos[\varphi_j + \varphi_k - \varphi_l - \varphi_m + k(r_j + r_k + s_{jk} - r_l - r_m - s_{lm})] .$$

In the case of only coherent scattering of the first order (the phases of echoes from individual scatterers are equal), for identical objects we have $I_{\text{coh}}^{(1)} = (N-1) I_{\text{in}}^{(1)}$ or $I_{\text{tot}} = N I_{\text{in}}^{(1)}$.

As it was mentioned above, $N(N+1)[N(N+1)/2+1]/4$ terms must be calculated to obtain the value of I_{tot}. This gives 1540 components for $N=10$ and 813450 for $N=50$.

Total backscattering intensity can be greater or smaller than its incoherent part because echoes from single centers can interfere constructively or destructively (coherent terms can be positive or negative). For estimation of an error connected with the assumption of the dominant role of incoherent scattering it is useful to introduce the following correction coefficient:

$$c_{\text{cor}} = I_{\text{in}}^{(1)} / I_{\text{tot}} .$$

For purely incoherent scattering its value is 1 and it decreases with rising contribution of coherent effects.

4. Scattering model with attenuation

Attenuation of the running wave takes place only inside the volume V on the way r_j' to the individual scatterer and on the way s_{jl} between two consecutive scatterers (Fig. 2)

$$r_j' = r_j (z_{\text{upp}} - z_j)/z_j ,$$

where r_j — a distance from the source to the jth bubble, z_j — its depth and z_{upp} — a depth of the upper boundary of the swarm of scatterers. Energetic coefficient of sound attenuation in bubbly water is expressed in Np/m and for identical bubbles has a form [7]:

$$\alpha = N\sigma_{e,R}/V,$$

where $\sigma_{e,R}$ is given by the formula (2.7).

Expressions (3.1)–(3.3) and (3.7) change their appearance:

$$p_j = A_j \frac{t_j}{r_j} \exp(ikr_j) \exp(-0.5\alpha r'_j), \tag{3.1}'$$

$$A_j = A_{0j} + \sum_{l \neq j}^{N} A_l \frac{t_l}{s_{jl}} \exp(iks_{jl}) \exp(-0.5\alpha s_{jl}). \tag{3.2}'$$

$$A_{0j} = \frac{A_0}{r_j} \exp(ikr_j) \exp(-0.5\alpha r'_j) \tag{3.3}'$$

$$a_{jj} = \frac{\rho_j}{r_j^2} \exp[i(\varphi_j + 2kr_j)] \exp(-\alpha r'_j) \quad \text{for} \quad j = l \tag{3.7}'$$

$$a_{jl} = \frac{\rho_j \rho_l}{r_j + r_l + s_{jl}} \exp\{i[\varphi_j + \varphi_l + k(r_j + r_l + s_{jl})]\} \exp[-0.5\alpha(r'_j + r'_l + s_{jl})] \quad \text{for } j \neq l$$

The effect of sound wave extinction was introduced to the model according to formulae (3.1)′–(3.7)′.

5. Numerical results

The first stage of calculations concerned N identical scatterers distributed both regularly and randomly in volume V with a given mean distance d between the neighbouring individuals. Sound attenuation was not included. The volume V was chosen as a parallelepiped with edges $n_1 d$, $n_1 d$ and $n_2 d$ ($n_1 * n_1 * n_2 = N$). In regular distributions bubbles were located in the nodes of a network, in random distributions each coordinate (x, y, z) of a scatterer was a random variable from the interval equal to the appropriate edge length determined for the regular case. In the random case the distances s_{jl} between all scatterers were tested and values smaller than diameter of a bubble were eliminated. Obtained values of backscattered field were averaged over 50 realisations.

In the first series of calculations the dependence of the scattered field on swarm density was investigated. For this purpose the value of d was being changed from $d=1$ cm to $d=10$ cm which resulted in change of total volume and, in consequence, in the bubble concentration. Various values of bubble number N (27 or 48), bubble radius a (10, 50, 75 and 100 μm) and swarm depth z_0 (1,5 and 10 m) were taken for each numerical calculation. Resonant frequency of a single bubble was chosen as a frequency of incident sound ($f=f_R$). Incoherent scattering of the first order practically depends neither on bubble

concentration nor on character of a distribution. In the random case it dominates for $d>2$ cm (Fig. 3). Incoherent term of the second order increases with decreasing volume for all kinds of distributions. For the densest packing ($d=1$ cm, i.e. $N/V=10^6/m^3$) this term contributed significantly — for random distribution it is even greater than the first order incoherent part. Regular distributions give the interference picture of I_{tot} with oscillations of order 30 dB which are connected with a vertical network dimension — large maxima occur at half wavelength and smaller — at quarter wavelength distance between horizontal layers of scatterers. It can be clearly seen on the diagram with horizontal axis and scale d/λ (Fig. 4).

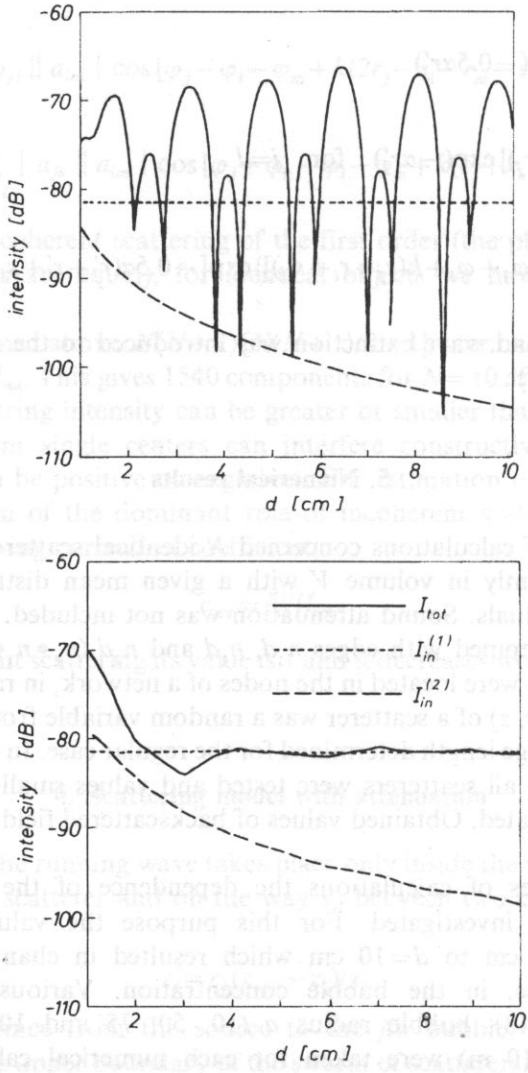

Fig. 3. Comparison of different order scattering effects for regular (upper) and random (lower) bubble distributions. $N=27$, $a=100$ μm, $z_0=10$ m.

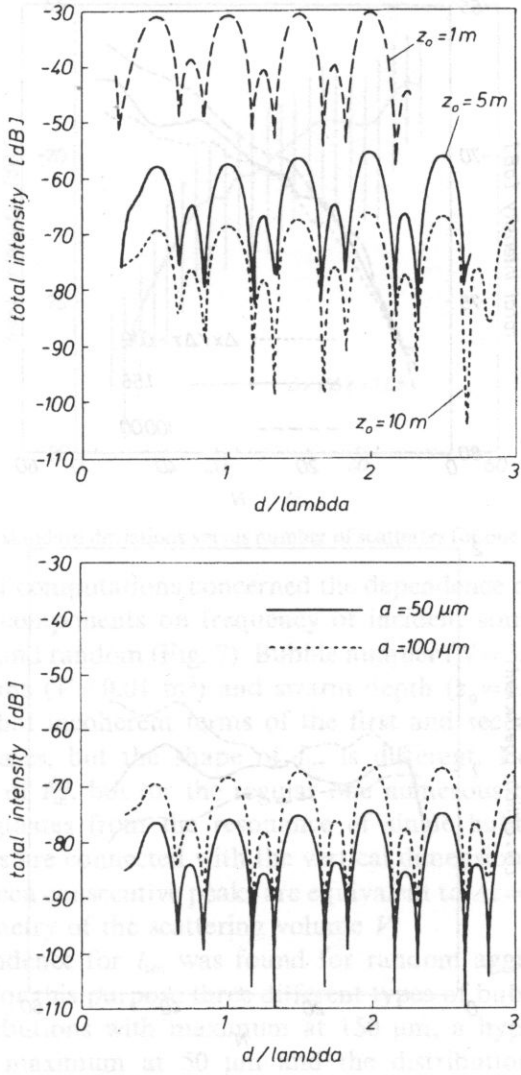

Fig. 4. Total intensity versus d/λ for regular bubble distribution for different swarm depths (upper) and different bubble radius (lower). $N=27$.

The second series of computation concerned the random distributions only. Values of scattering volume ($V=0.01$ m^3), bubble radius ($a=100$ μm) and swarm depth ($z_0=5$ m) were fixed and bubble number N was varied. Calculations were carried out for seven different ratios $\Delta x/\Delta z$ of scattering volume: from $\Delta x/\Delta z=0.1$ — tall and narrow parallelepiped (in practice it is equivalent to narrow beam and long pulse) to $\Delta x/\Delta z=100$ — low and broad (broad beam and short pulse). Fig. 5 shows the dependence of the total intensity and correction coefficient on number of bubbles in given volume for three chosen geometries. Apart from an obvious fact that

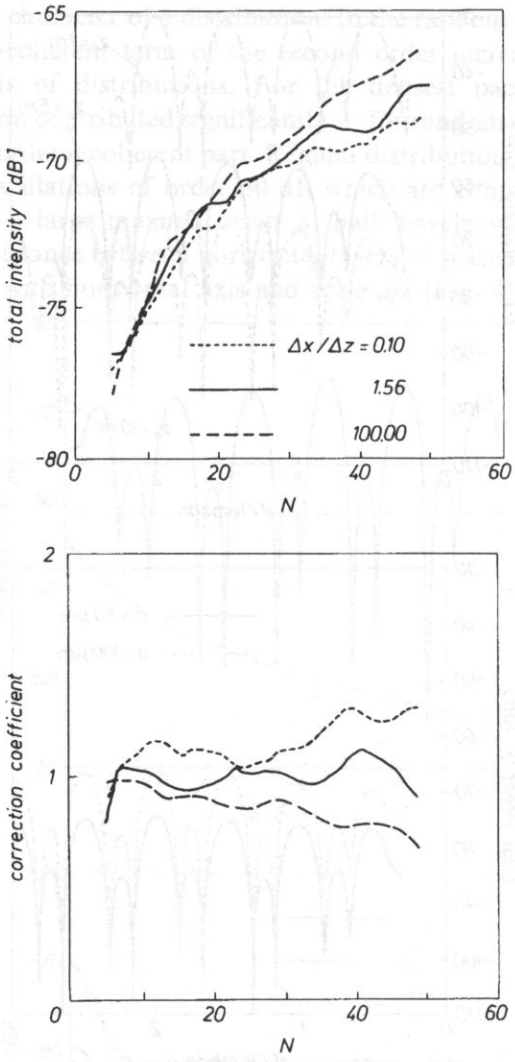

Fig. 5. Dependence of total intensity (upper) and correction coefficient (lower) on number of bubbles enclosed in volume $V=0.01$ m^3 for three geometries. Bubbles distributed randomly, averaging over 100 realisations.

intensity increases with increasing number of scatterers, we can see the tendency that with flattening and broadening of the parallelepiped the total echo rises and correction coefficient falls. It means that coherent scattering becomes more substantial, what is obvious for 2-dimensional (flat) scattering systems. The shape of these curves is very uneven despite increasing the number of averaged realisations to 100, because of large changeability of succesive realisations (see standard deviations in Fig. 6).

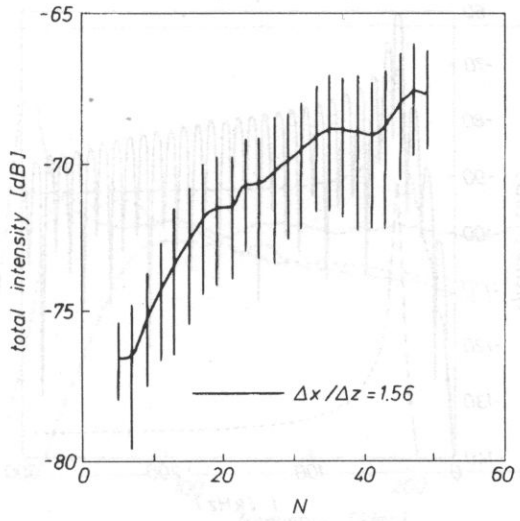

Fig. 6. Total intensity with standard deviations versus number of scatterers for one of geometries from Fig. 5.

The third series of computations concerned the dependence of the total backscattered signal and its components on frequency of incident sound for two types of distribution: regular and random (Fig. 7). Bubble number ($N=32$), its radius ($a=100$ μm), scattering volume ($V=0.01$ m^3) and swarm depth ($z_0=5$ m) were fixed. The comparison shows that incoherent terms of the first and second order are almost identical for both cases, but the shape of I_{tot} is different. For the random case I_{tot} repeats the form of $I_{\text{in}}^{(1)}$, but for the regular one numerous maxima appear. The largest of them originates from the resonance of single bubble f_R (according to formula (2.2)), others are connected with the vertical dimension Δz of the scattering area. Distances between consecutive peaks are equivalent to $\Delta z=\lambda/2$ and they change together with a geometry of the scattering volume V.

Analogous dependence for I_{tot} was found for random aggregations of bubbles with various radii. For this purpose three different types of bubble size spectra were chosen: Gauss distributions with maximum at 150 μm, a hypothetical power law distribution with a maximum at 50 μm and the distribution of KOLOBAEV and DEKTEREV [2] describing natural marine population of gas bubbles:

(1) $n(a)\sim\exp[-(a-\bar{a})^2/2\sigma^2]$ $\bar{a}=150$ μm (Gauss),

(2) $n(a)\sim\begin{cases} a & \text{for } a<50 \text{ μm} \\ a^{-3} & \text{for } a>50 \text{ μm} \end{cases}$ (power law),

(3) $n(a)\sim a^{-3}\exp(-3\bar{a}/a)$ $\bar{a}=15$ μm (KOLOBAEV and DEKTEREV [2]).

All these distributions were normalized to give $N_{\text{tot}}=50$. Fig. 8 illustrates the dependence $I_{\text{tot}}(f)$ (upper part) for particular distributions (lower part). It can be seen that for aggregation of bubbles with different radii the resonant maximum of I_{tot} is

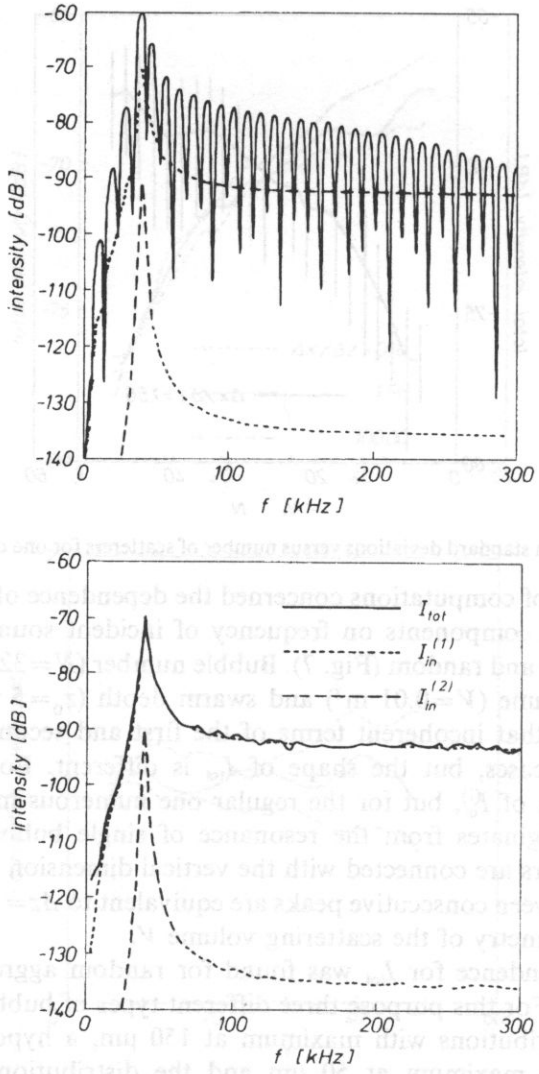

Fig. 7. Frequency dependence of the total backscattering energy and its components for regular (upper) and random (lower) bubble distributions. $N=32$, $a=100$ μm, $z_0=5$ m, $V=0.01$ m^3, $\Delta x/\Delta z=1.56$.

broadened in comparison with the case of bubbles with the same radii (see Fig. 7) and the shift of maximum in size spectrum causes the shift of resonant peak of backscattered intensity according to reverse proportionality of f and a_R. Additionally, the bigger bubbles dominate in the aggregation, the higher is the level of I_{tot} in the nonresonant area (large frequencies).

The dependence of the calculated backscattered intensity without and with attenuation on the linear dimension of swarm is shown in Fig. 9. For very small volumes V (i.e. huge bubble densities N/V) the attenuated field is about tens of dB

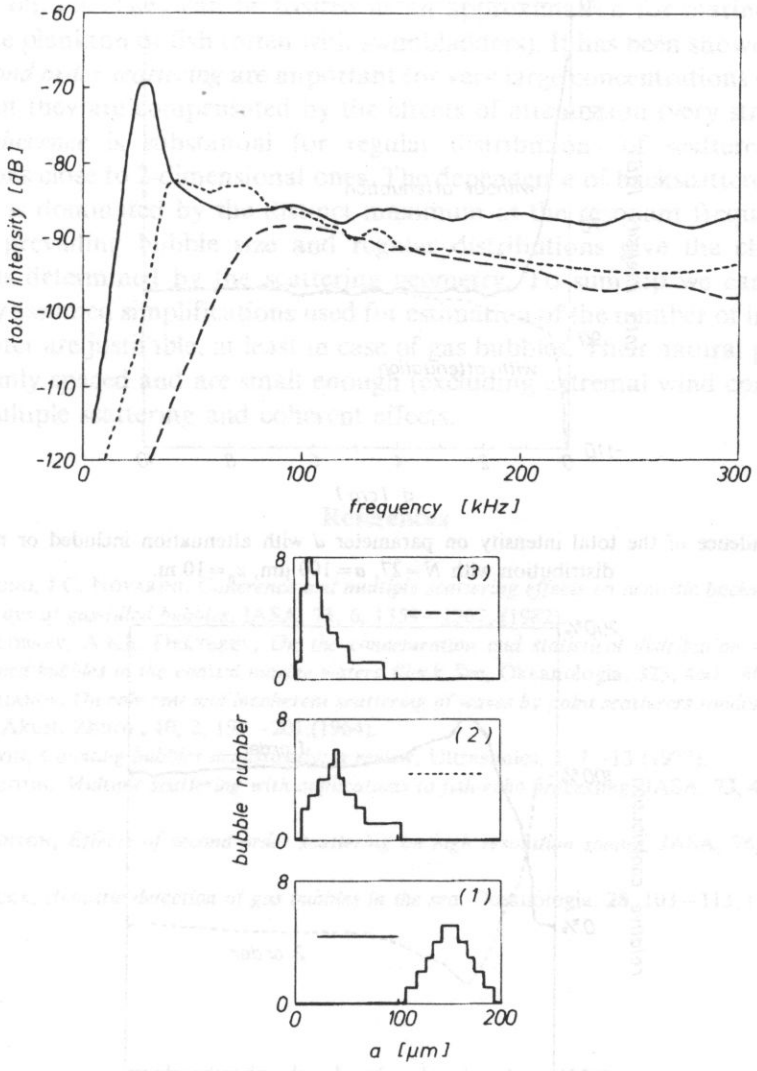

Fig. 8. Frequency dependence of the total backscattering energy (upper) for different kinds of bubble size spectra (lower).

smaller than the unattenuated one. A comparison of this diagram with the dependence of the first and second order terms of backscattered energy on the linear size of aggregation (Fig. 10) shows that the range of large attenuation is the same as the range of domination of the second order scattering. Therefore we can conclude that strong attenuation eliminates the second order effects. On the other hand, in the range of moderate bubble densities (under $10^4/m^3$), the role of both attenuation and interaction diminishes and these effects become negligible.

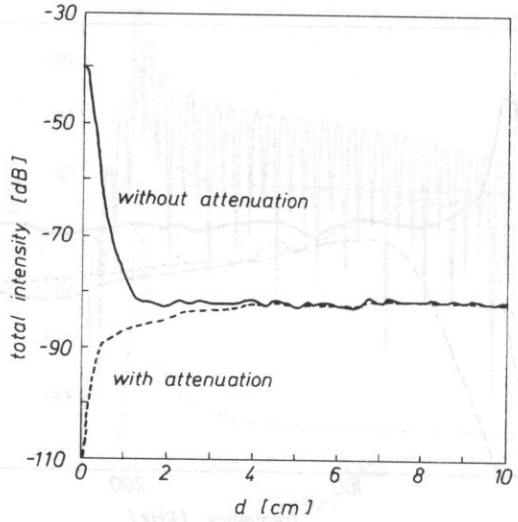

Fig. 9. Dependence of the total intensity on parameter d with attenuation included or not. Random distribution with $N=27$, $a=100$ μm, $z_0=10$ m.

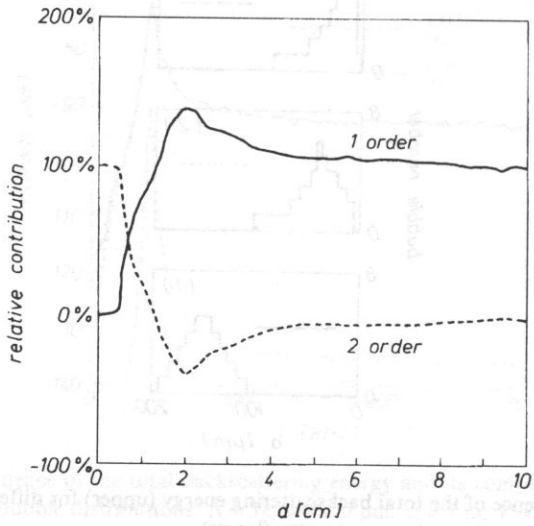

Fig. 10. Relative contribution of the first and second order scattering effects to total intensity for random set of bubbles. $N=27$, $a=100$ μm, $z_0=10$ m.

6. Summary

On the basis of numerical model describing the total field of signals backscattered on the collection of isotropic scatterers an attempt of verification of two fundamental assumptions of echosounding was made. Free gas bubbles were chosen as modelled

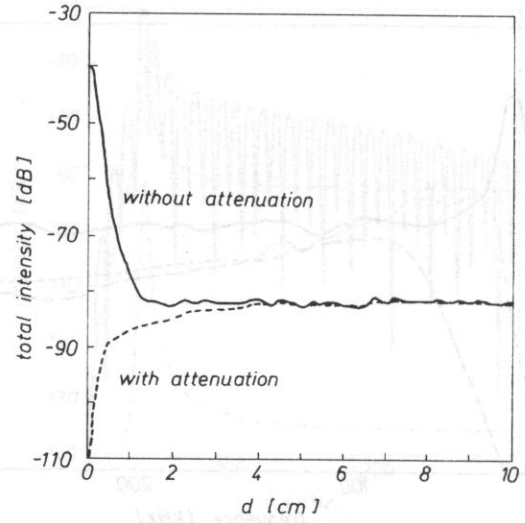

Fig. 9. Dependence of the total intensity on parameter d with attenuation included or not. Random distribution with $N=27$, $a=100$ μm, $z_0=10$ m.

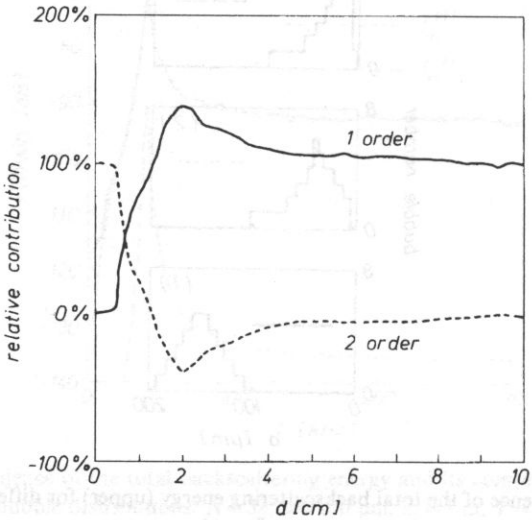

Fig. 10. Relative contribution of the first and second order scattering effects to total intensity for random set of bubbles. $N=27$, $a=100$ μm, $z_0=10$ m.

6. Summary

On the basis of numerical model describing the total field of signals backscattered on the collection of isotropic scatterers an attempt of verification of two fundamental assumptions of echosounding was made. Free gas bubbles were chosen as modelled

scattering objects. They can be treated as an approximation for marine biological objects like plankton or fish (often with swimbladders). It has been shown that terms of the *second order scattering* are important for very large concentrations of the order $10^6/m^3$, but they are compensated by the effects of attenuation (very strong in that area). *Coherence* is substantial for regular distributions of scatterers and for aggregations close to 2-dimensional ones. The dependence of backscattered signal on frequency is dominated by the distinct maximum at the resonant frequency of the single or prevailing bubble size and regular distributions give the characteristic oscillations determined by the scattering geometry. To sum up we can state that commonly assumed simplifications used for estimation of the number of intrusions in the sea water are justifable, at least in case of gas bubbles. Their natural populations are randomly spaced and are small enough (excluding extremal wind conditions) to neglect multiple scattering and coherent effects.

References

[1] D.R. Bruno, J.C. Novarini, *Coherence and multiple scattering effects on acoustic backscattering from linear arrays of gas-filled bubbles*, IASA, **71**, 6, 1359–1367, (1982).

[2] P.A. Kolobaev, A.Kh. Dekterev, *On the concentration and statistical distribution of the sizes of wind-formed bubbles in the coastal marine waters Black Sea*, Okeanologia, **323**, 460–465, (1992).

[3] B.F. Kurianov, *On coherent and incoherent scattering of waves by point scatterers randomly distributed in space*, Akust. Zhurn., **10**, 2, 195–201,(1964).

[4] H. Medwin, *Counting bubbles acoustically: a review*, Ultrasonics, **1**, 7–13 (1977).

[5] T.K. Stanton, *Multiple scattering with applications to fish-echo processing*, JASA, **73**, 4, 1164–1169, (1983).

[6] T.K. Stanton, *Effects of second-order scattering on high resolution sonars*, JASA, **76**, 3, 861–866, (1984).

[7] J. Szczucka, *Acoustic detection of gas bubbles in the sea*, Oceanologia, **28**, 103–113, (1989).